Probing the hadron-quark phase transition in twin stars with f-modes

David Álvarez Castillo

Institute of Nuclear Physics PAS
Cracow, Poland

INCUBATOR OF SCIENTIFIC EXCELLENCE

UNIVERSIDAD AUTÓNOMA DE NUEVO LEÓN

Uniwersytet Wrocławski

RESEARCH UNIVERSITY
EXCELLENCE INITIATIVE

XVII Polish Workshop on Relativistic Heavy-Ion Collisions:
Phase diagram and Equation of State of strongly interacting matter
December 14, 2024

dalvarez@ifj.edu.pl

CREDO
THE QUEST FOR THE UNEXPECTED

EINSTEIN TELESCOPE

compstar

Outline

- A brief introduction to the physics of compact stars and their relation to the QCD phase diagram.
- The compact star mass twins scenario.
- f-mode detection and EoS constraints.
- Outlook and perspectives.

Motivation

- New channels of multi-messenger observations like gravitational radiation from merger events of binary systems of compact stars or radio and X-ray signals from isolated pulsars allow to study their most basic structural properties like mass, radius, compactness, cooling rates and compressibility of their matter.

- Nuclear measurement and experiments have narrowed the Equation of State (EoS) uncertainty in the lowest to intermediate density range.

- Violent, transient energetic emissions are associated not only with the strong magnetic fields and extreme gravity in the proximity of NS but with explosive, evolutionary stages often triggered by mass accretion from companion stars. It is expected that are f-modes are excited in many of these astrophysical processes.

The Extraordinary Core of a Neutron Star

A neutron star's core is so dense that physicists aren't sure what happens inside. Researchers can't recreate the conditions in the lab, and even the theory of nuclear matter is of limited help. Here are some of the main ideas.

TRADITIONAL VIEW OF A NEUTRON STAR

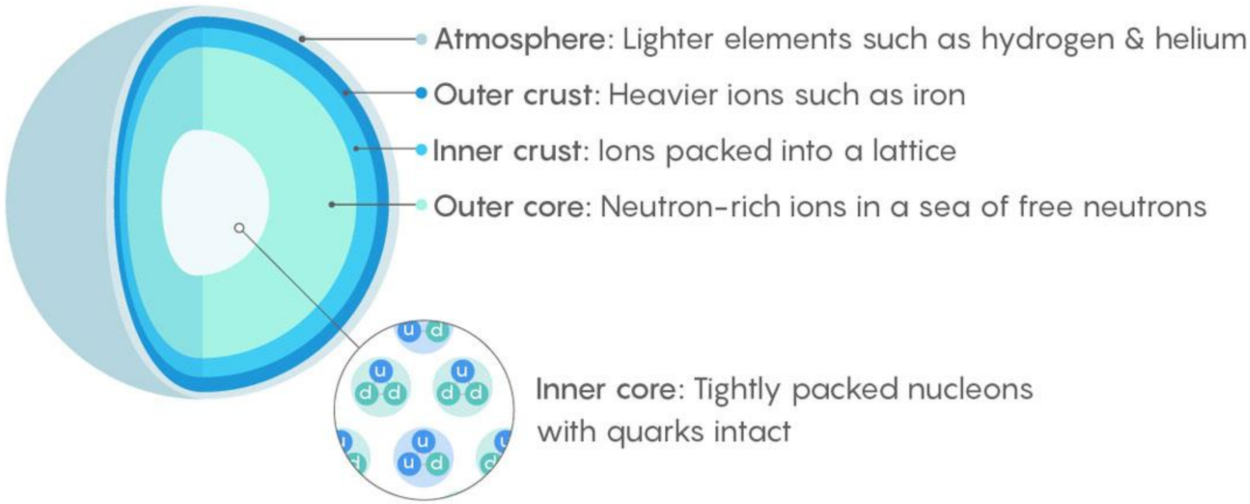

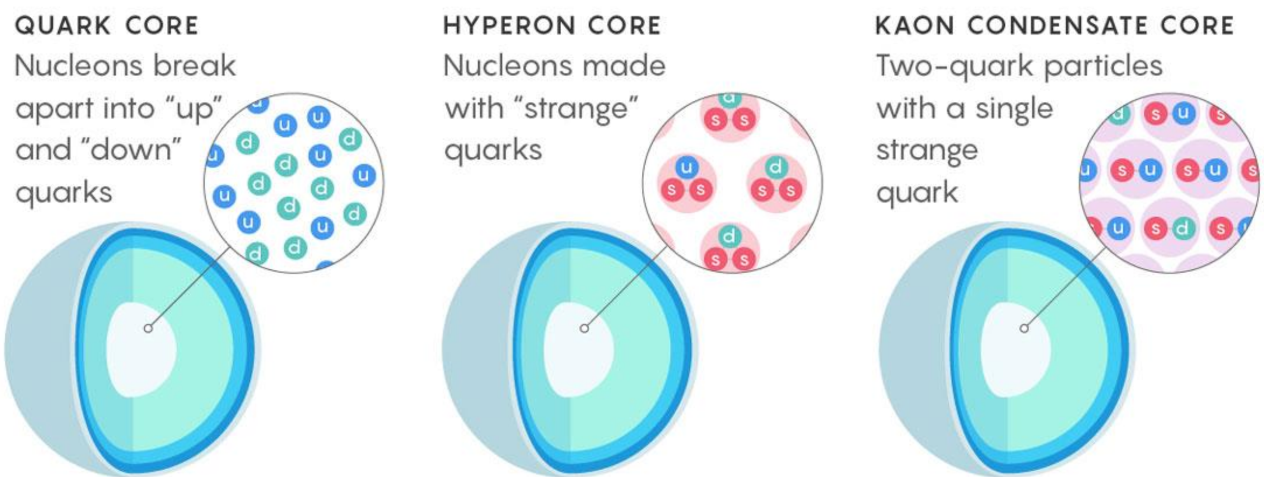

Critical Endpoint in QCD

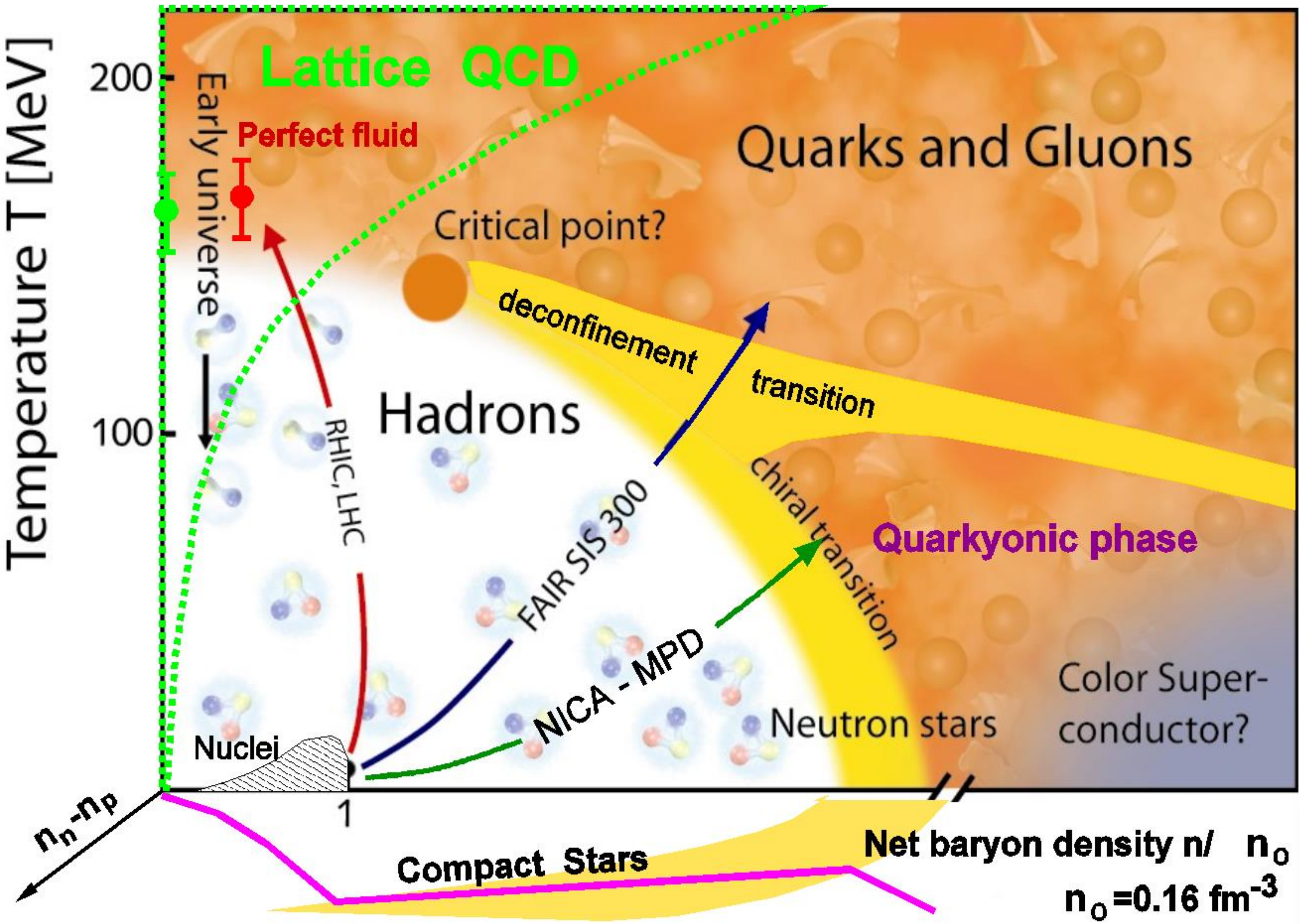

Compact Star Sequences
(M-R ⇔ EoS)

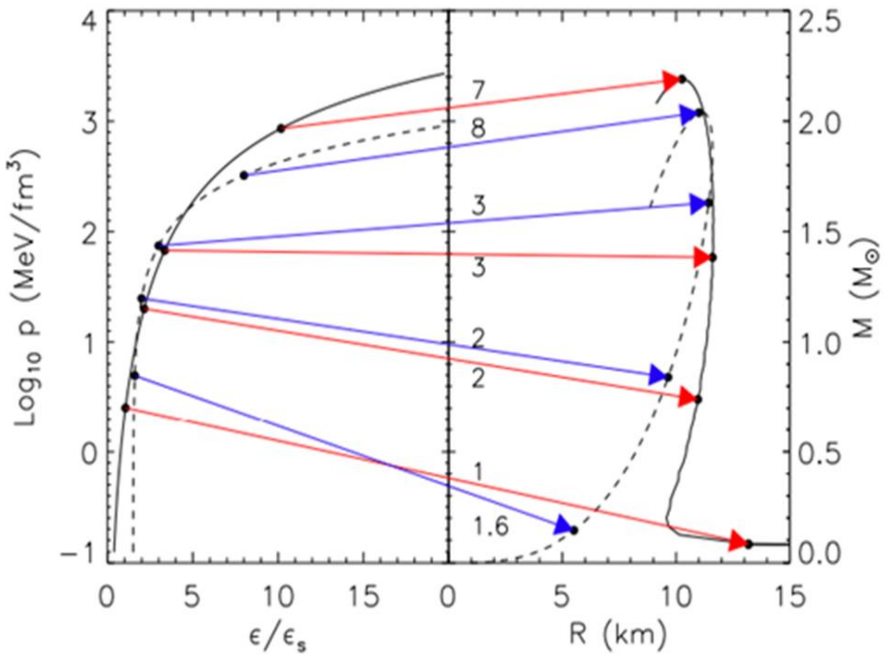

James Lattimer,
Annu. Rev. Nucl. Part. Sci. 62,
485 (2012), arXiv:1305.3510

- TOV Equations

$$\frac{dp}{dr} = -\frac{(\varepsilon + p/c^2)G(m + 4\pi r^3 p/c^2)}{r^2(1 - 2Gm/rc^2)}$$

- Equation of State (EoS)

$$\frac{dm}{dr} = 4\pi r^2 \varepsilon \qquad p(\varepsilon)$$

Compact Star Mass Twins and the AHP scheme

- First order PT can lead to a stable branch of hybrid stars with quark matter cores which, depending on the size of the "latent heat" (jump in energy density), can even be disconnected from the hadronic one by an unstable branch → "**third family of CS**".

- Measuring two **disconnected populations** of compact stars in the M-R diagram would represent **the detection of a first order phase transition** in compact star matter and thus the indirect proof for the existence of a **critical endpoint (CEP) in the QCD phase diagram**!

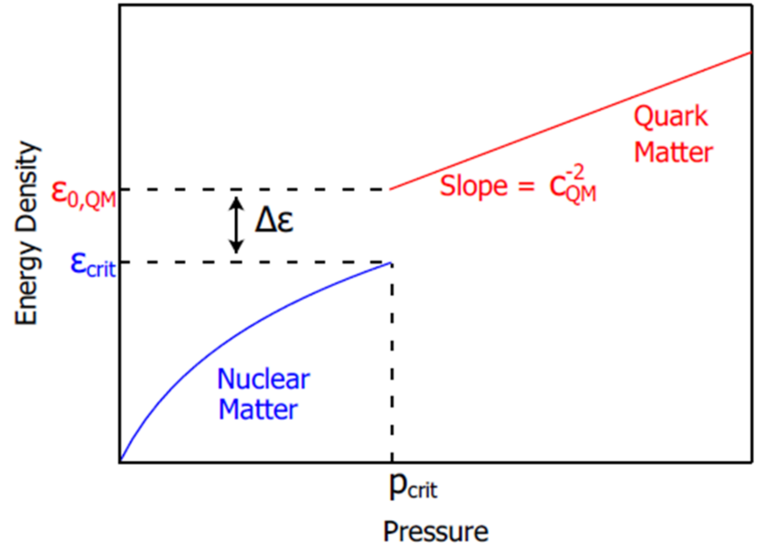

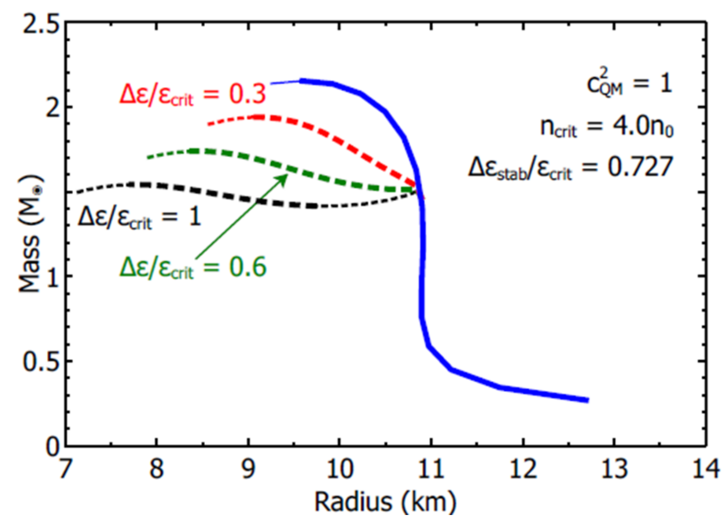

Alford, Han, Prakash,
Phys. Rev. D 88, 083013 (2013)
arxiv:1302.4732

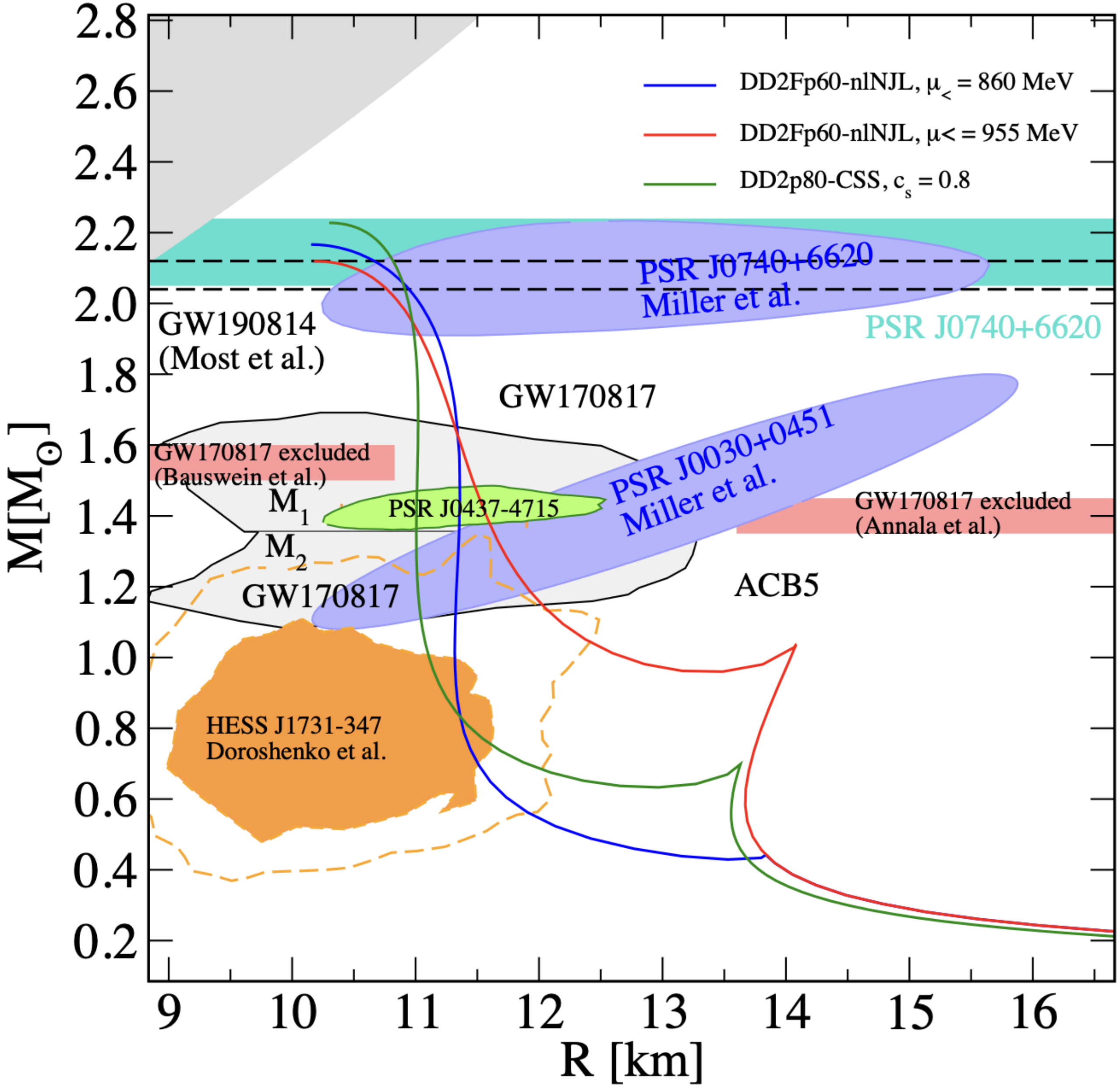

DD2Fp60-nlNJL, $\mu_<$ = 860 MeV
DD2Fp60-nlNJL, μ< = 955 MeV
DD2p80-CSS, c_s = 0.8
PSR J0740+6620
Miller et al.
PSR J0740+6620
GW190814
(Most et al.)
GW170817
GW170817 excluded
(Bauswein et al.)
M_1
PSR J0437-4715
PSR J0030+0451
Miller et al.
GW170817 excluded
(Annala et al.)
M_2
GW170817
ACB5
HESS J1731-347
Doroshenko et al.
M[$M_\odot$]
R [km]

QCD trace anomaly at the core of twin stars

$$\Delta = \frac{1}{3} - \frac{c_s^2}{\gamma}, \quad \Delta' = c_s^2\left(\frac{1}{\gamma} - 1\right)$$

$$d_c = \sqrt{\Delta^2 + (\Delta')^2}$$

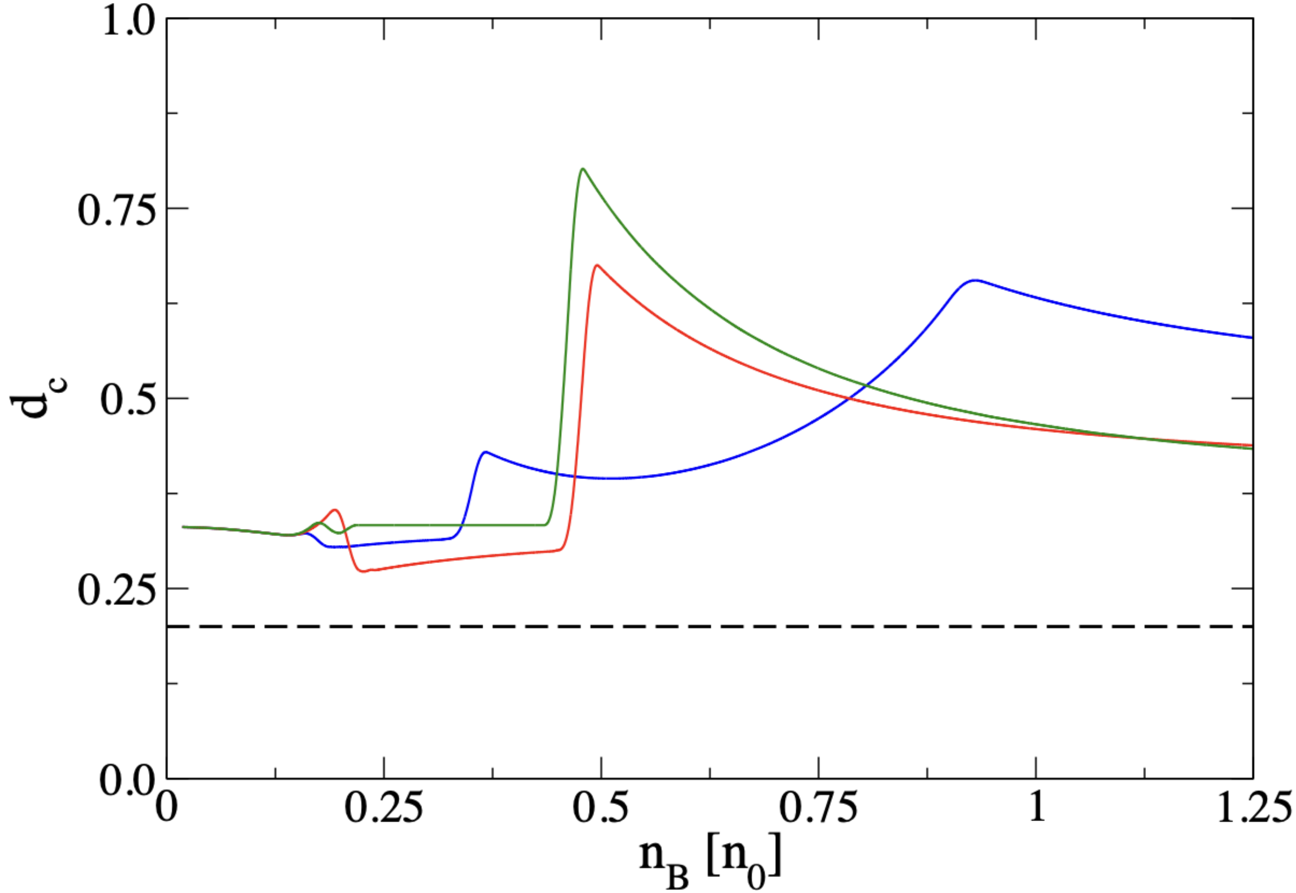

For discussion, see arXiv:2408.11614, arXiv:2407.15486, and Nat Commun 14, 8451 (2023)

Thermal Compact Star Twins

Rep. Prog. Phys. **81** (2018) 056902

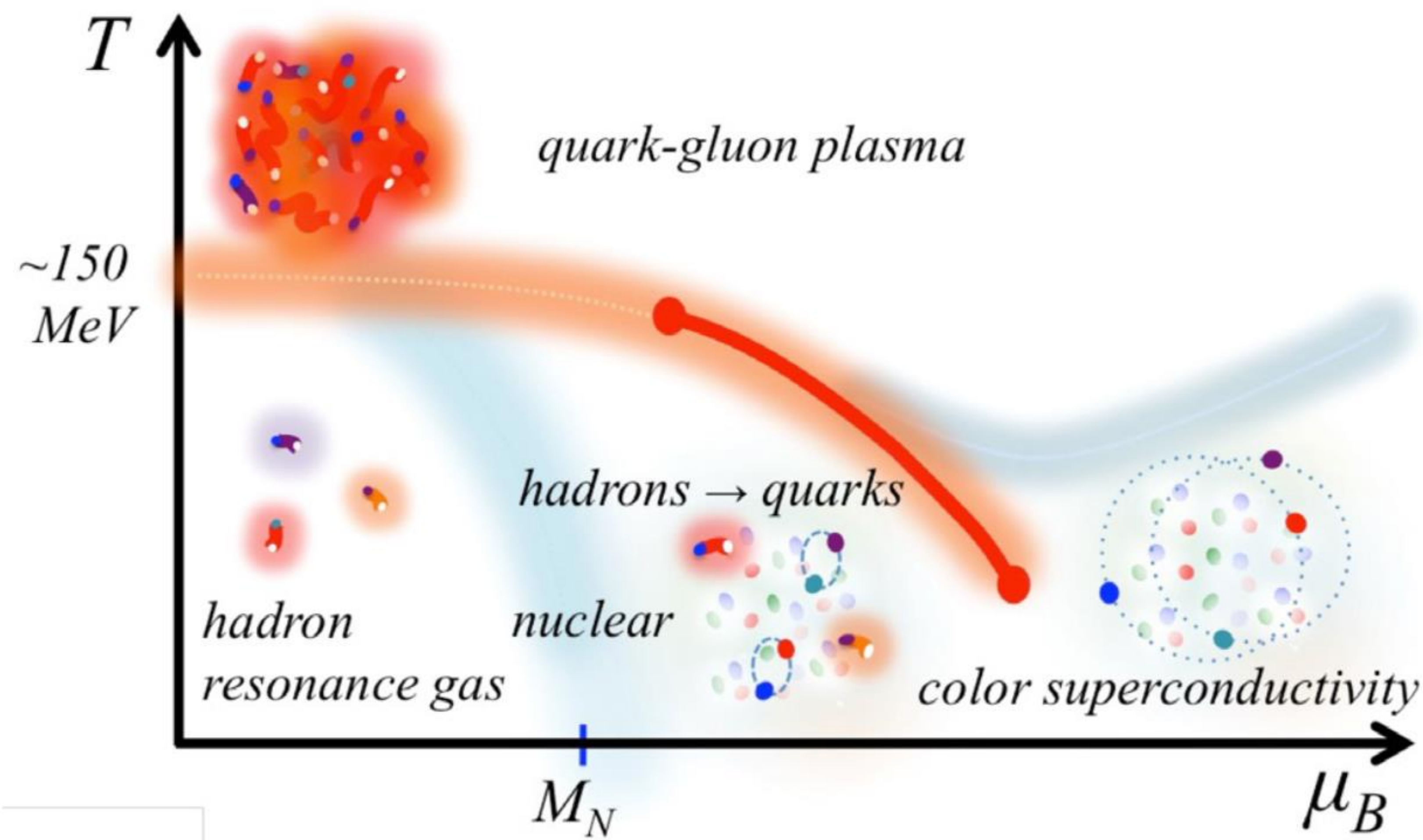

Thermal Compact Star Twins

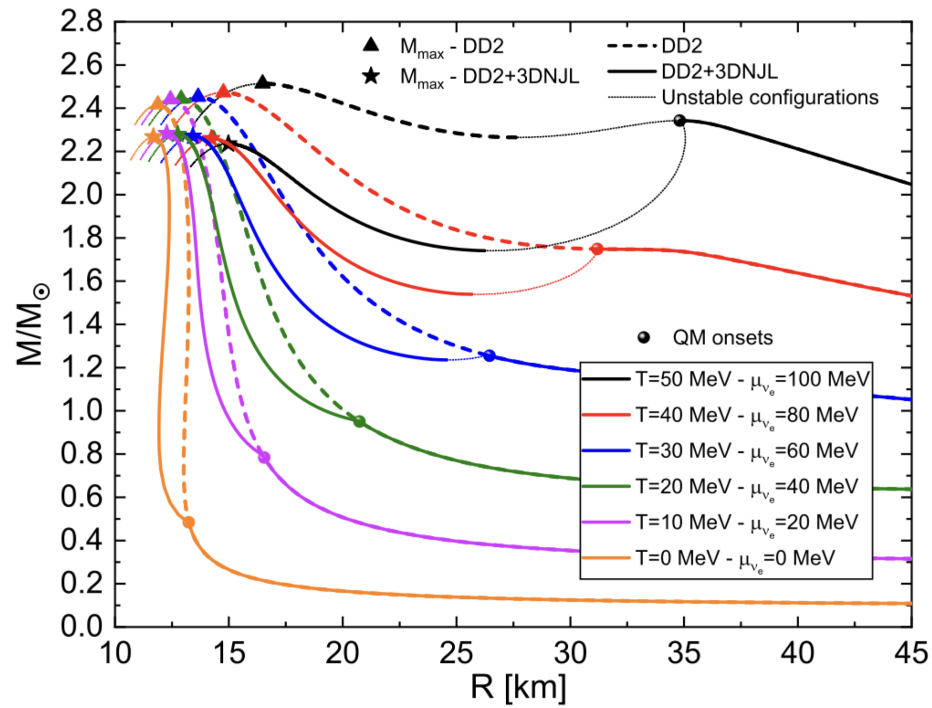

FIG. 11. Mass-radius relations from hybrid EOSs for different values of T and μ_{ν_e}. Short-dashed lines correspond to crust + DD2 EOSs while solid lines also include QM. For all the cases, dotted lines show the unstable regions. Solid dots display the QM onsets and star (triangle) symbols indicate the M_{max} locations for hybrid (hadronic) EOSs.

J.P. Carlomagno, G.A. Contrera, A.G. Grunfeld, and D. Blaschke
Phys. Rev. D 109, 043050 (2024), arXiv:2312.01975

Observables in the quark-hadron phase transition

- Proton neutron star collapse and Shock formation
- Explosion mechanism of massive stars
- Observable in neutrino signal:
- Resolvable in (Super-K, Icecube) for a galactic supernova

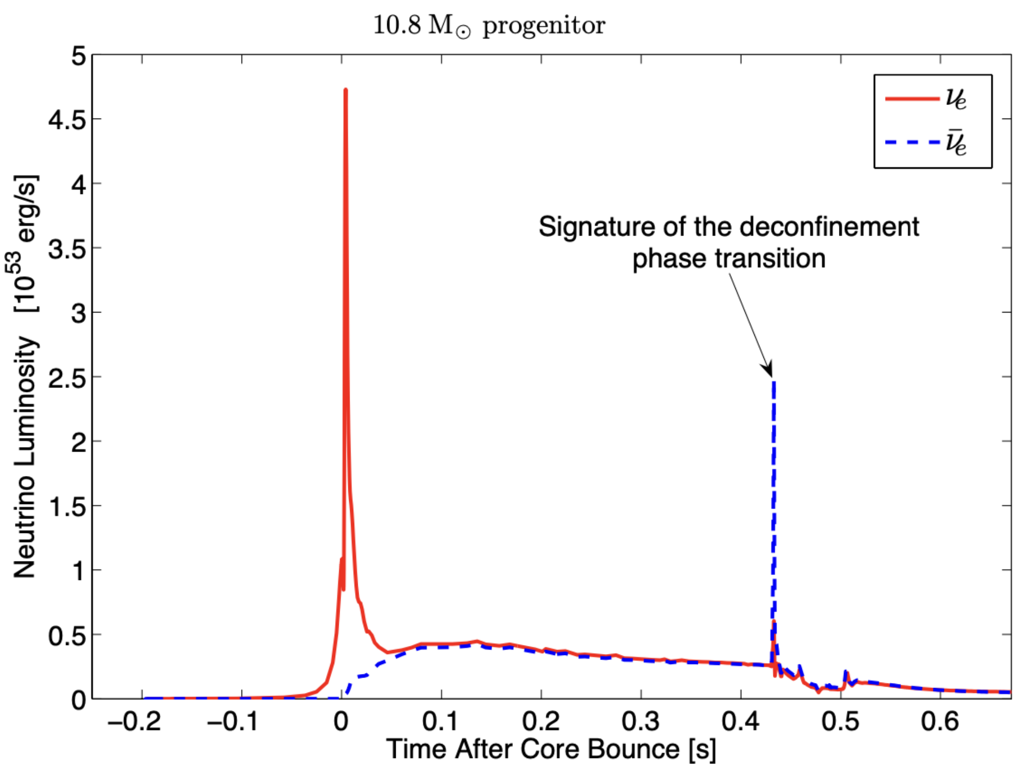

Sagert & T.F. et al. (2009), PRL 102, 081101
Dasgupta & T.F. et al. (2010), PRD 81
T.F. et al. (2011), ApJS 194, 39

The remnant hybrid star

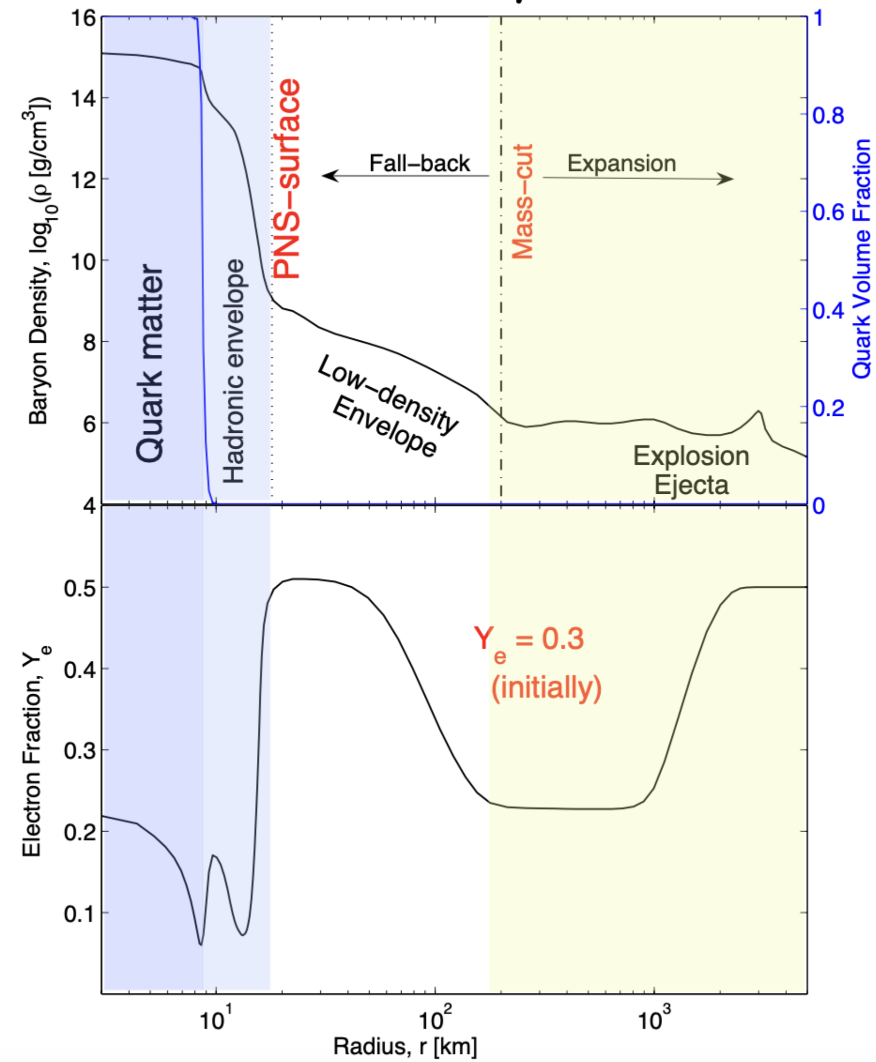

Credit: Tobias Fischer

Implications on eccentric and isolated millisecond pulsar populations

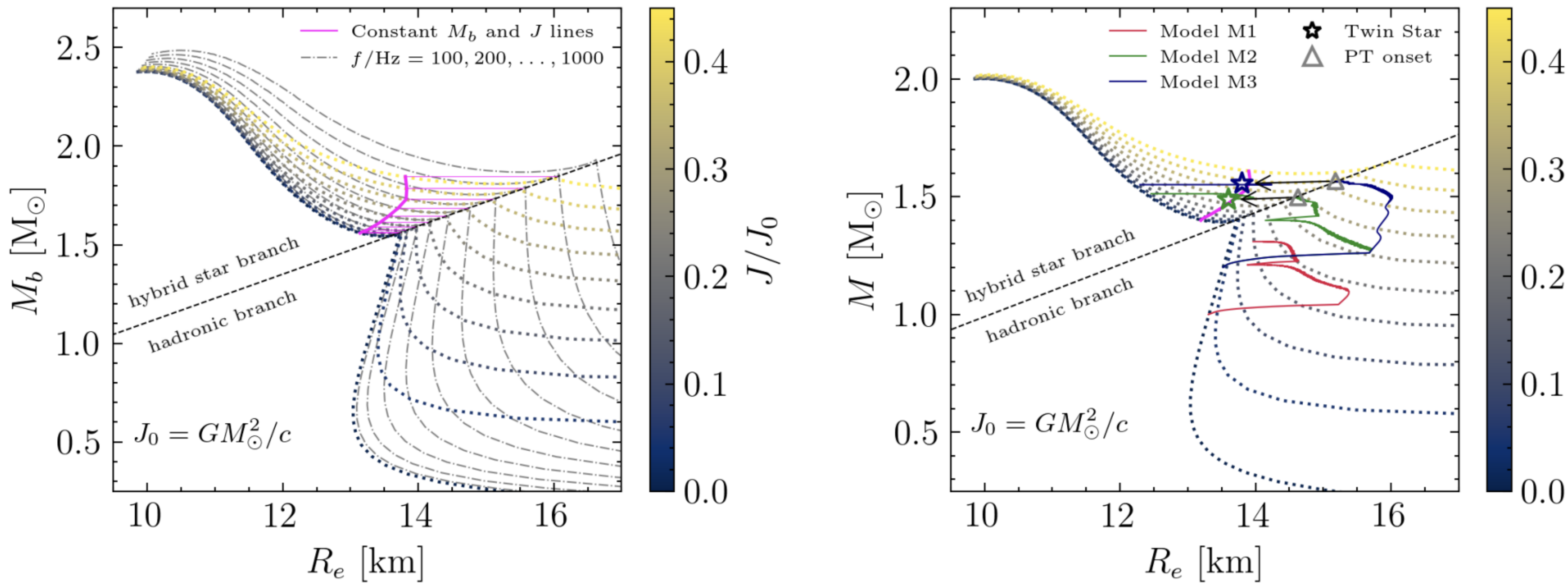

Fig. 1: *Left Panel*: Baryonic mass vs. equatorial radius. Dotted and dot-dashed curves indicate lines of constant angular momentum and constant frequency respectively. The black dashed line highlights the points of maximum stability in the hadronic branches, signaling the onset of a phase transition (PT). Thin, horizontal magenta lines show trajectories where angular momentum (J) and baryonic mass (M_b) are conserved. The thick magenta curve connects points on the hybrid star branches that can be reached through a collapse conserving both J and M_b. *Right Panel*: Similar to the left panel, but with the y-axis representing gravitational mass. Star markers denote the endpoint trajectories for direct (M2) and delayed (M3) collapse models. Here, the arrows are inclined because gravitational mass, unlike baryonic mass, is not conserved during the PT.

S. Chanlaridis et al. - arXiv:2409.04755

Implications on eccentric and isolated millisecond pulsar populations

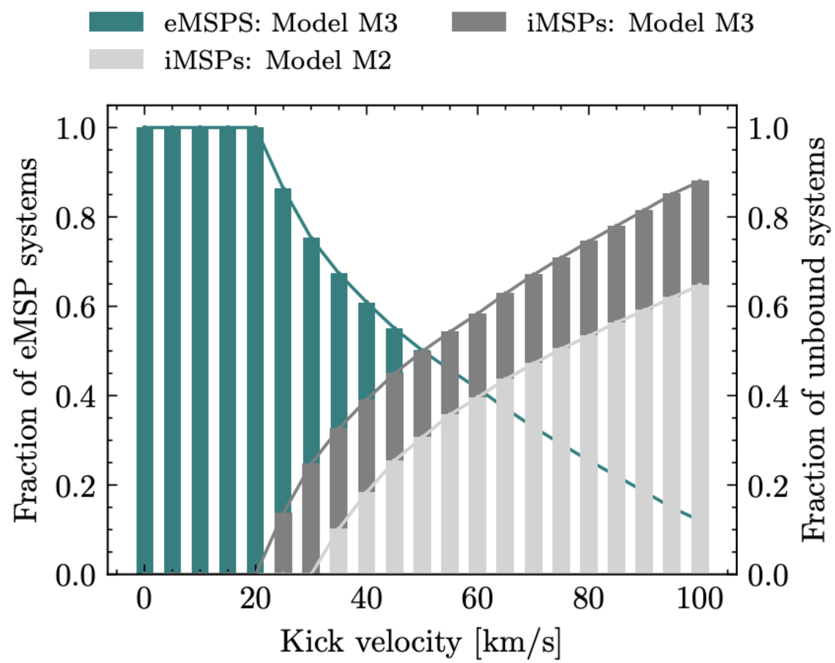

Fig. 6: Expected fraction of eMSPs (left y-axis) and iMSPs (hatched gray-colored bars, right y-axis) as a function of kick velocity, assuming a mass defect of $\Delta M = 0.016\,M_\odot$. For iMSPs, we consider those systems with eccentricities greater than unity. Model M2 cannot create eccentric systems due to rapid recircularization of the orbit.

S. Chanlaridis et al. - arXiv:2409.04755

The Crust of Twin Compact Stars

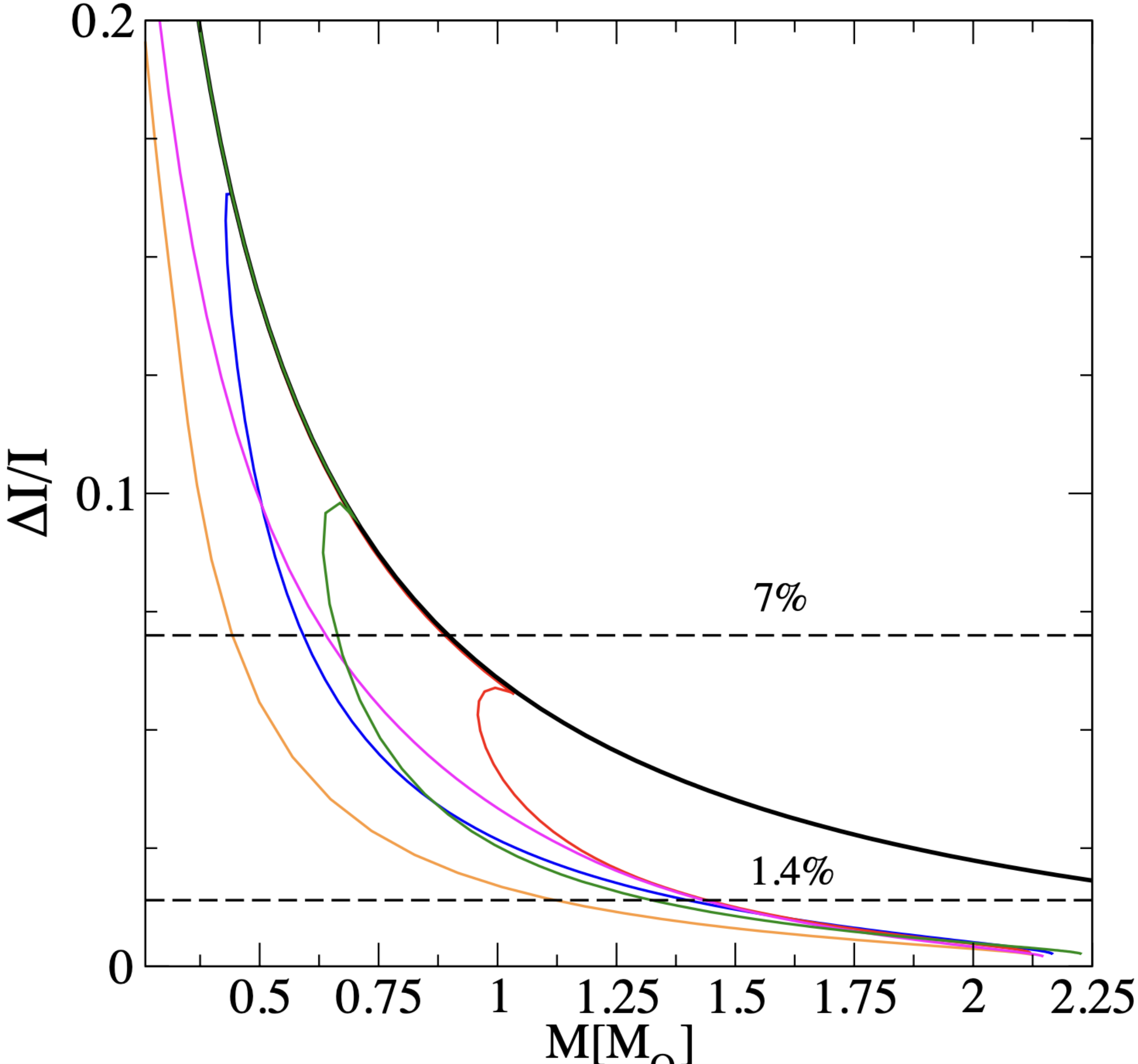

Gravitational Waves from NS

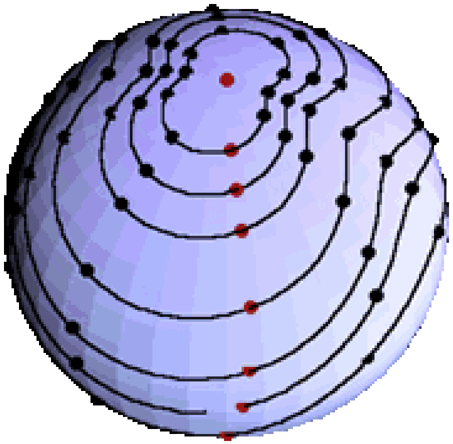

Credit: C. Hanna and B. Owen

Credit: CERN/Indico

PC: cosmicexplorer.org/sensitivity

- Non-radial QNMs raised from time varying quadrupole deformations are source of GWs.

  - fundamental (f) mode,
    - no node, probe for mean density,(1 kHz < f < 3kHz)
  - pressure (p) mode,
    - Sound speed, (5 kHz < f < 10kHz)
  - gravity (g) mode,
    - (50 Hz < f < 500 Hz)
- R-mode, for rotating stars only.
  - Viscosity, (0.5 kHz < f < 2kHz)
- Space-time (w) mode.
  - 5 kHz< f

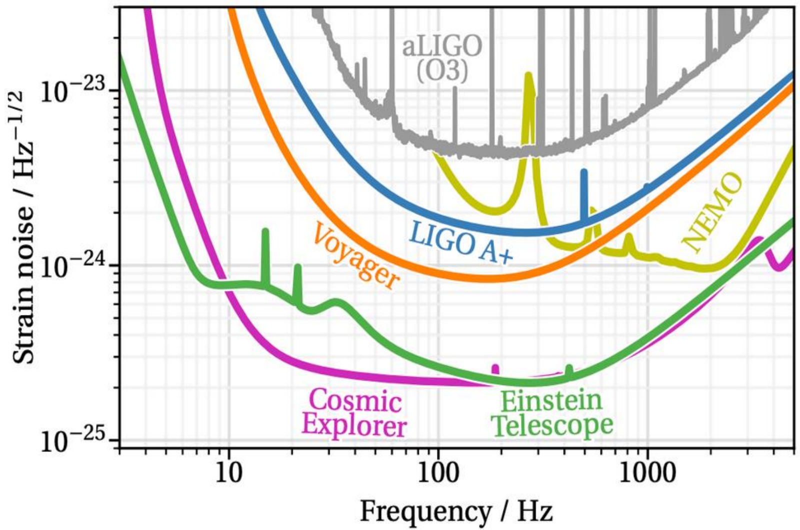

Stellar Properties

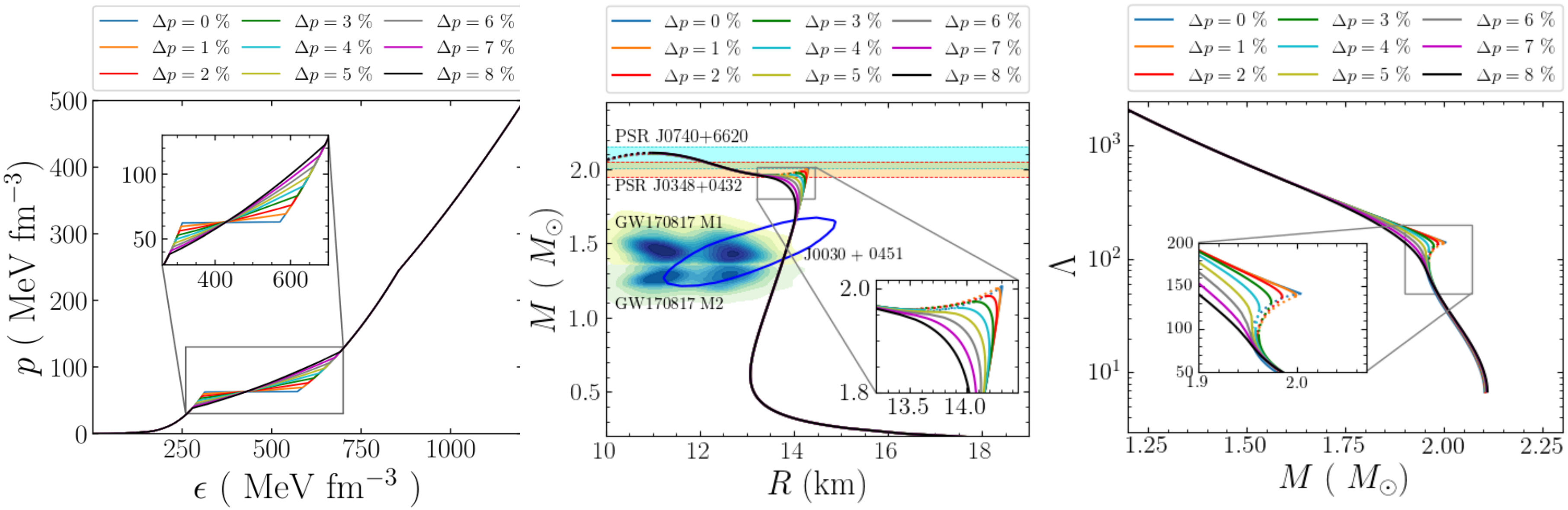

- The second and third family merge to form a single branch for Δp > 4% .
- Precise measurement of *M-R* required for detection of twin star.
- The jump ΔΛ (if any) can be measured ~15 % (< 90% CI) with next-generation GW detectors (P. Landry & K. Chakravarti , arXiv:2212.09733 ,2022).

David Alvarez-Castillo, Bikram Keshari Pradhan, Debarati Chatterjee – arXiv:2309.08775
Monthly Notices of the Royal Astronomical Society, Vol 531, Issue 4, Pag 4640–4655 (2024)

f-mode characteristics

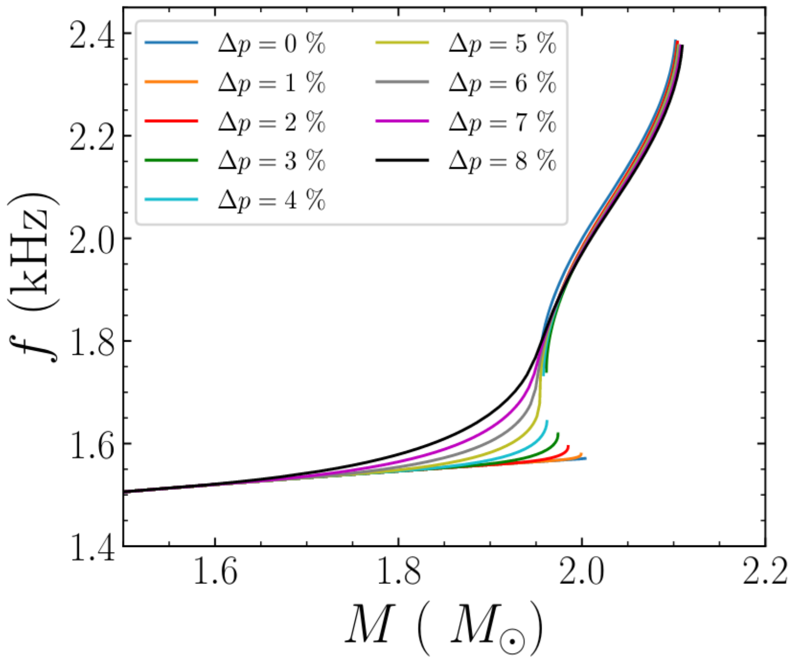

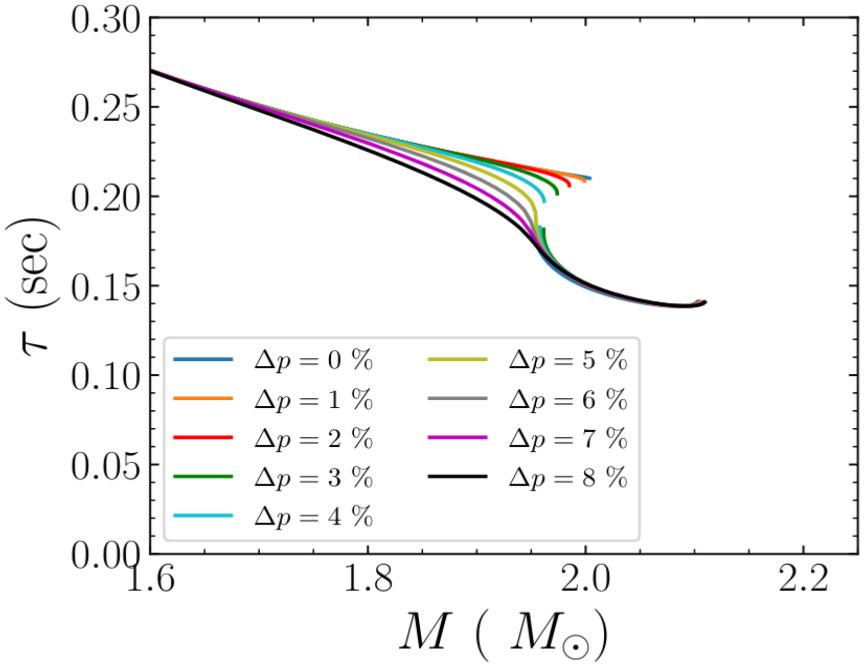

- f-mode characteristics are obtained within ***General relativistic*** formalism.
- Sudden increase (decrease) in the frequency (damping time) observed with appearance of twin star.
- Detections of f-mode GWs from compact stars with known mass may reveal the presence of twin stars.
- Simultaneous measurement of *M-f* (from binary system) can be used to comment on twin stars.

David Alvarez-Castillo, Bikram Keshari Pradhan, Debarati Chatterjee – arXiv:2309.08775
Monthly Notices of the Royal Astronomical Society, Vol 531, Issue 4, Pag 4640–4655 (2024)

Asteroseismology and Universal Relations

- URs among f-mode characteristics (f, τ_f or $\omega=2\pi f+1/\tau_f$) and NS observables.

$$f(\text{kHz}) = a_r + b_r\sqrt{\frac{M}{R^3}}$$

Empirical relations (EOS dependent)

$$\text{Re}(M\omega) = a_0 + a_1\left(\frac{M}{R}\right) + a_2\left(\frac{M}{R}\right)^2$$

$$\text{Im}(M\omega) = b_0\left(\frac{M}{R}\right)^4 + b_1\left(\frac{M}{R}\right)^5 + b_2\left(\frac{M}{R}\right)^6$$

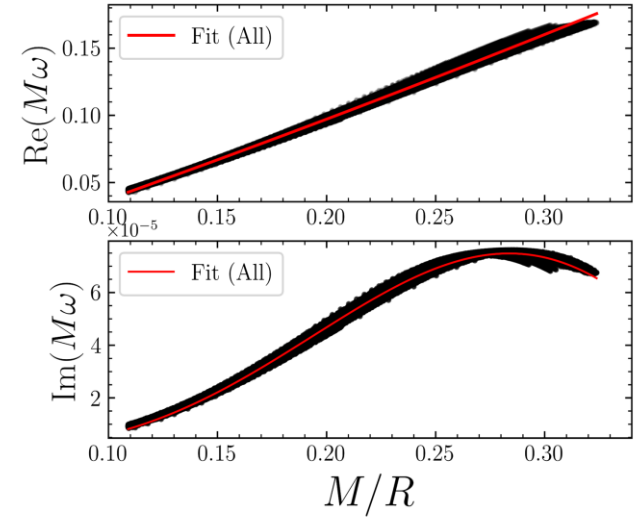

	Re(Mω)		Im(Mω)
a_0	-0.027±9 × 10^{-5}	b_0	(9.81 ± 0.004) × 10^{-2}
a_1	0.610 ± 0.0015	b_1	(−4.444 ± 0.003) × 10^{-1}
a_2	0.049±0.002	b_2	(4.91 ± 0.0045) × 10^{-1}

- Scaled Universal relations are more useful.
- The URs can be used for EoS inference.
- URs involving tidal deformability have also been examined.

David Alvarez-Castillo, Bikram Keshari Pradhan, Debarati Chatterjee – arXiv:2309.08775
Monthly Notices of the Royal Astronomical Society, Vol 531, Issue 4, Pag 4640–4655 (2024)

Compact star observables from f-mode observations: the role of UR Uncertainty

- ❖ Determination under the assumption that *f*, ⍰ are measured precisely.
- ❖ Errors on UR results uncertainties on *M*-*R*.

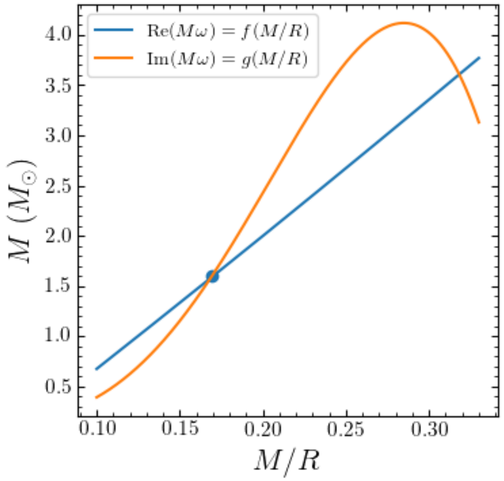

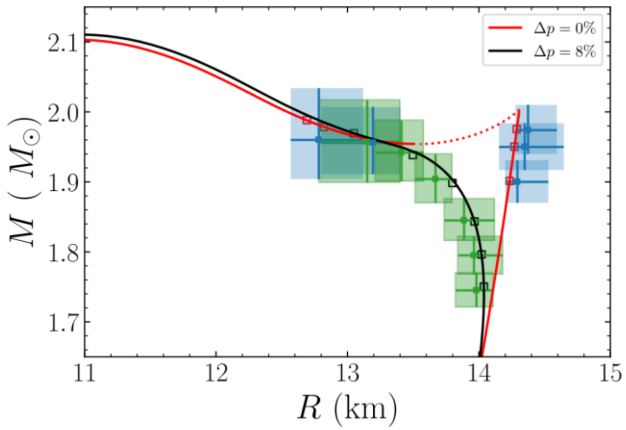

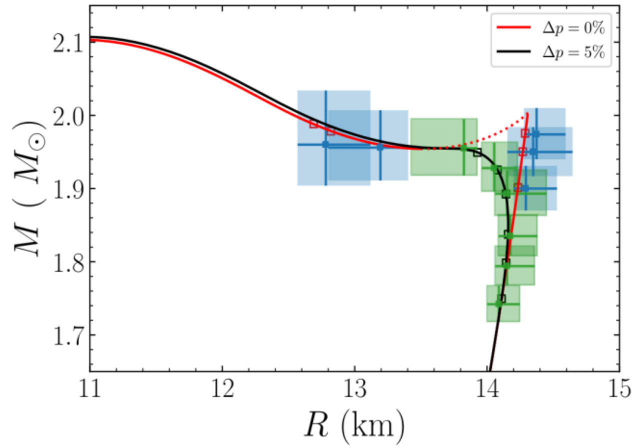

- ★ The presence of the twins maybe confirmed with exact measurement of *f, and* ⍰ .
- ★ The unstable branch of Δp = 0% can be distinguished from the connecting stable branch of Δp =8%.
- ★ Differentiating among Δp =0% and Δp =5% is more challenging.

David Alvarez-Castillo, Bikram Keshari Pradhan, Debarati Chatterjee – arXiv:2309.08775
Monthly Notices of the Royal Astronomical Society, Vol 531, Issue 4, Pag 4640–4655 (2024)

Inclusion of Observational Uncertainties

- F-mode being excited during pulsar glitches. All the energy radiated through GW.
- The burst waveform is modelled as an exponentially damped oscillation.

$$h(t) = h_0 \exp\left(-t/\tau_f\right) \sin\left(2\pi\nu_f t\right), \;\; t > 0$$

(B.J. Owen,2010, Ho et al. 2020)

$$h_0 = 4.85\times10^{-17}\sqrt{\frac{E_{\rm gw}}{M_\odot c^2}}\sqrt{\frac{0.1{\rm sec}}{\tau_f}}\frac{1{\rm kpc}}{d}\left(\frac{1{\rm kHz}}{\nu_f}\right)$$

f-modes GW

$$E_{\rm gw} = E_{\rm glitch} = 4\pi^2 I \nu^2 (\frac{\Delta\nu}{\nu})$$

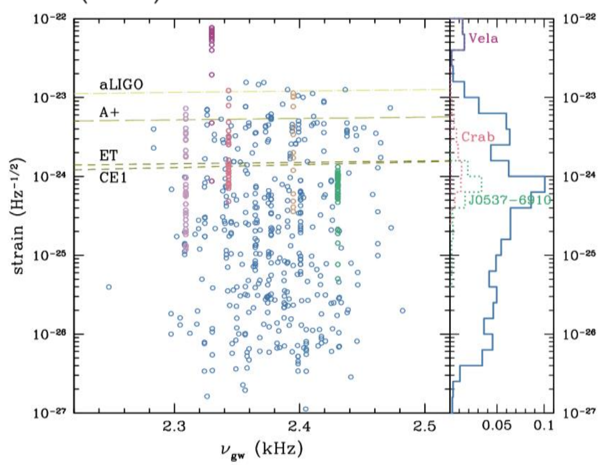

Ho et al ,PRD 101, 103009 (2020)

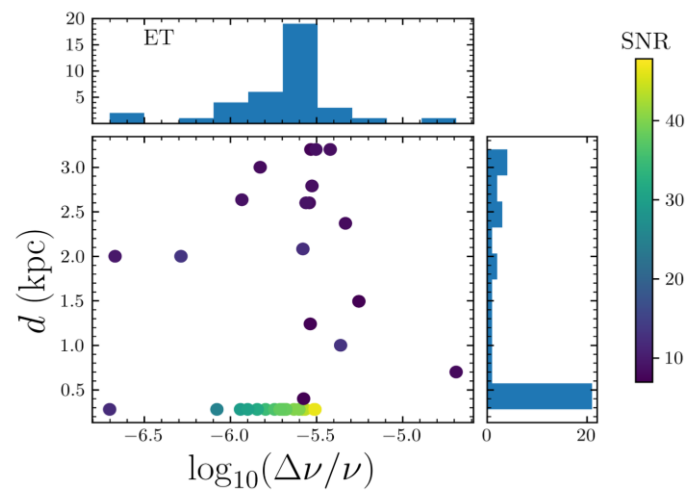

B. K. Pradhan, D. Pathak, and D. Chatterjee, *ApJ* **956** 38, (2023)

- B. Abbott et al.,LVC, *ApJ* **874** 163, 2019.
- R. Abbott et al.,LVK, PhRvD, 104, 122004, 2021.
- R. Abbott, et al., LVK, arXiv:2210.10931, 2022.
- R. Abbott, et al., LVK, arXiv:2203.12038, 2022.
- D. Lopez et al., PhRvD, 106, 103037, 2022

David Alvarez-Castillo, Bikram Keshari Pradhan, Debarati Chatterjee – arXiv:2309.08775
Monthly Notices of the Royal Astronomical Society, Vol 531, Issue 4, Pag 4640–4655 (2024)

Inclusion of Observational Uncertainties

- Glitching pulsars data taken from the Jodrell Bank Glitch catalogue.
- Spin frequency, distance (d) and sky position to each pulsar are assign from ATNF Pulsar Catalogue.
- Consider few random mass configurations with an assumed EOS model .
- Then f-mode frequency, damping time, moment of inertia to pulsars from the assume EoS model.

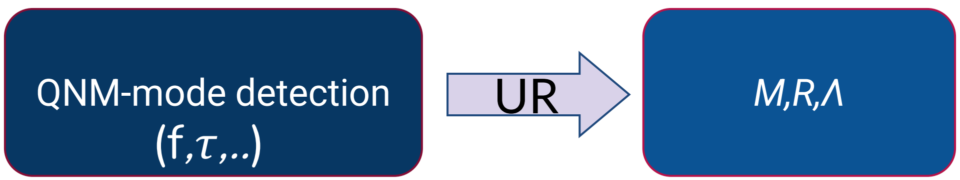

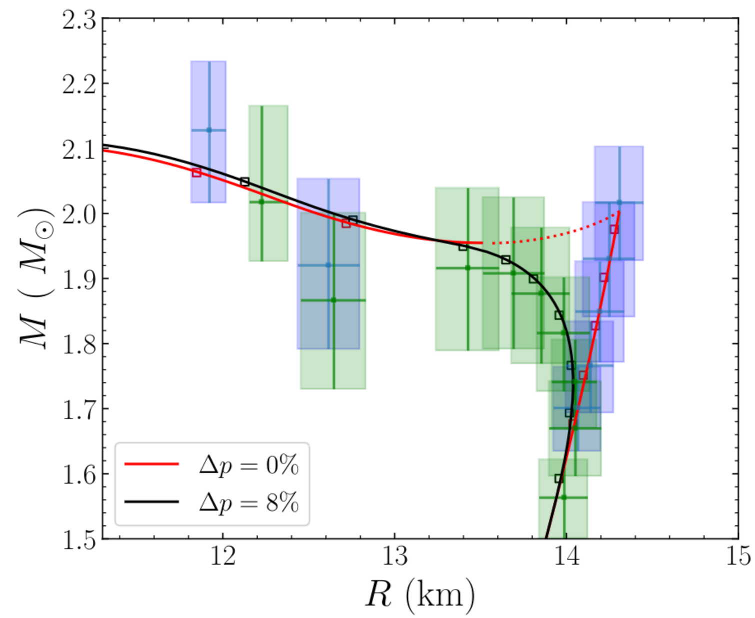

- The measurement of *R* from f-mode observation may confirm the presence of twins.
- More challenging for low mass twins. However, we have more observations at low masses.
- Differentiating the nature of Δp is more challenging.

David Alvarez-Castillo, Bikram Keshari Pradhan, Debarati Chatterjee - arXiv:2309.08775

Outlook

- Multi-messenger astronomy and collider experiments will continue probing the properties of dense matter.
- Bayesian Analysis and Machine Learning methods are useful for estimation of unknown physical parameters.
- f-mode oscillation of hybrid stars and twin stars involving the “pasta phase” has been investigated.
- Re-examination of the asteroseismology problem considering the twin stars.
- Precise f-mode measurement provides suitable scenario for twin star detection.
- Compact star crusts studies and measurements are work in progress.

Outlook

- f-mode GW detection with next-generation GW offers a promising scenario for confirming the existence of the twin stars.
- Distinguishing the nature of hadron-quark crossover phase transition requires further studies. Interestingly, accretion onto neutron stars can potentially excite fundamental modes in connection with neutrino emissions allowing for probing for phase transitions, see arXiv:2311.15992.
- Consideration of the effect of rotation and magnetic fields can potentially improve this study.
- A detailed Bayesian study is in progress to constrain the pasta phase parameters from f-mode/binary observation.

Gracias

Einstein Telescope

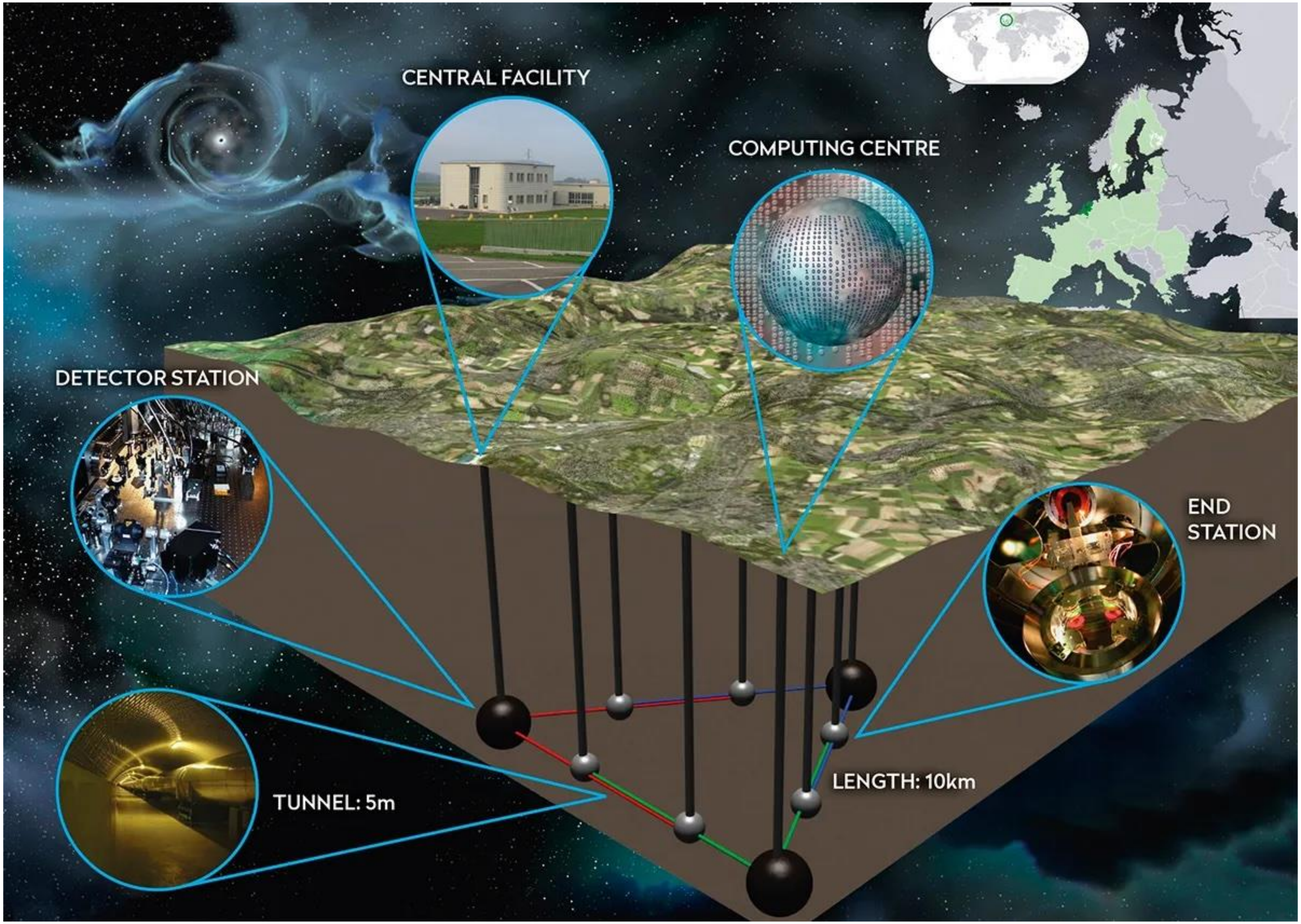

Einstein Telescope

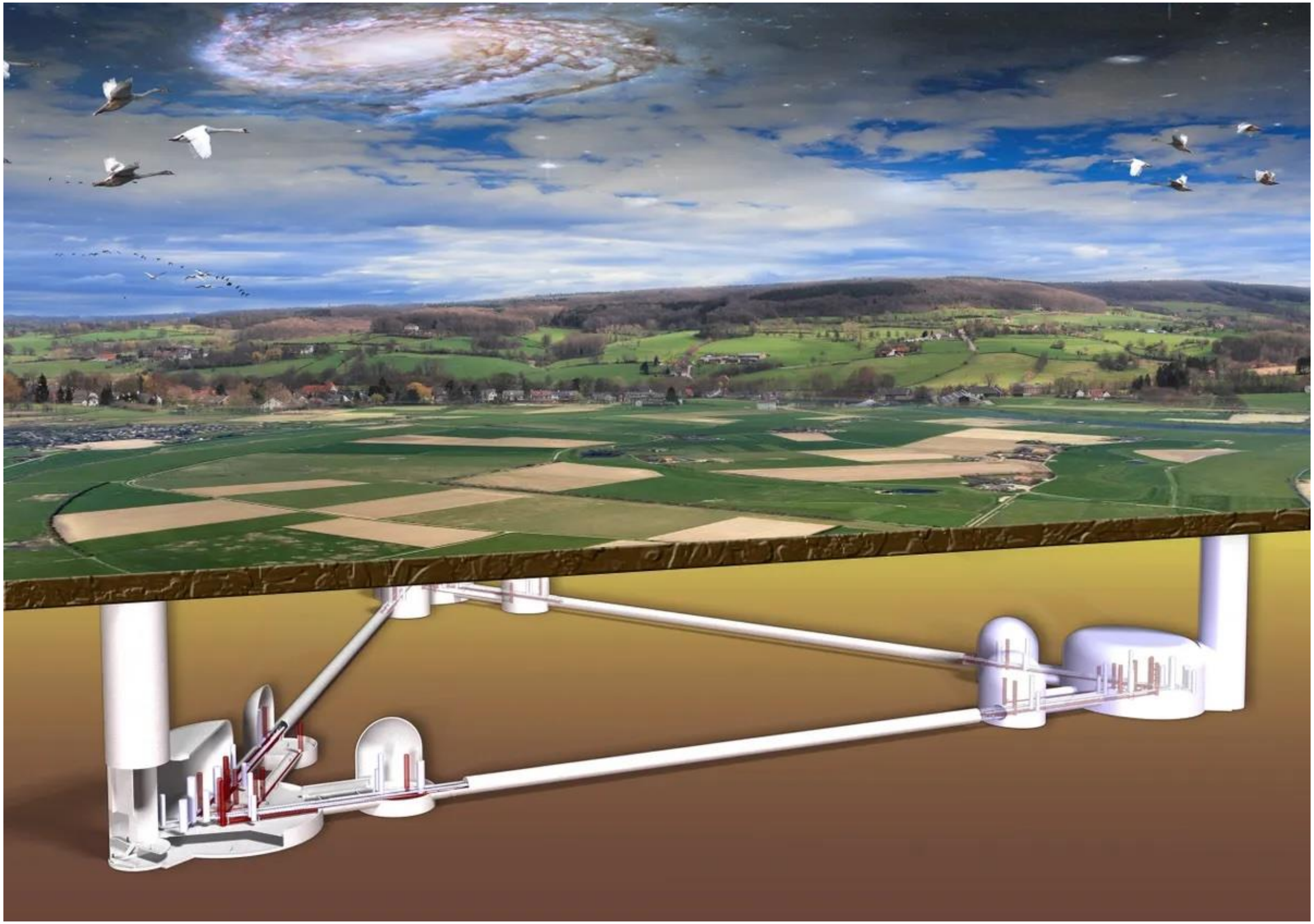

KAGRA

ET EINSTEIN TELESCOPE

MeerKAT

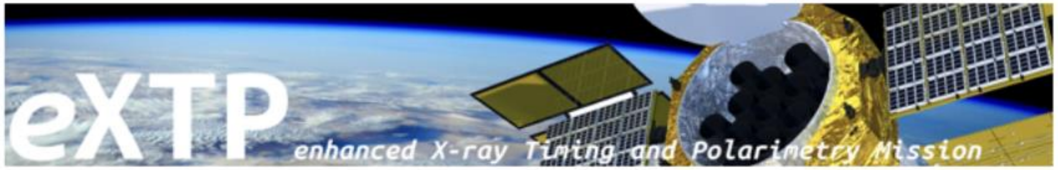

Neutron Star Equation of State

The energy per nucleon in neutron star core matter is given by:

$$\begin{aligned} E_{\rm tot}(n,\{x_i\}) &= E_{\rm b}(n,x_p)+E_{\rm lep}(n,x_e,x_\mu)\ , \\ E_{\rm b}(n,x_p) &= E_0(n)+S(n,x_p) \\ E_{\rm lep}(n,x_e,x_\mu) &= E_e(n,x_e)+E_\mu(n,x_\mu)\ , \end{aligned}$$

where $n = n_p + n_n$ is the total baryon density and $x_i = n_i/n$, $i = p, e, \mu$ are the fractions of protons, electrons and muons, respectively. The baryonic part is very well described by the parabolic approximation w.r.t. the asymmetry

$$\alpha = \frac{n_n - n_p}{n_n + n_p} = 1 - 2x_p,$$

resulting in $S(n, x_p) = (1 - 2x_p)^2 E_s(n)$. The leptonic contribution is a sum of the Fermi gas expressions for the contributing leptons $l = e, \mu$

$$E_l(n,x_l) = \frac{1}{n}\frac{p_{F,l}^4}{4\pi^2}\left[\sqrt{1+z_l^2}\left(1+\frac{z_l^2}{2}\right) - \frac{z_l^4}{2}\mathrm{Arsinh}\left(\frac{1}{z_l}\right)\right]\ ,$$

where $z_l = m_l/p_{F,l}$. For massless leptons ($z_l \to 0$), this expression goes over to

$$E_l(n,x_l)\big|_{m_l=0} = \frac{1}{n}\frac{p_{F,l}^4}{4\pi^2} = \frac{3}{4}\left(3\pi^2 n\right)^{1/3} x_l^{4/3}\ .$$

Charge neutrality and β-equillibrium

Under neutron star conditions charge neutrality holds,

$$x_p = x_e + x_\mu \ .$$

The $\beta-$ equilibrium with respect to the weak interaction processes $n \to p + e^- + \bar{\nu}_e$ and $p + e^- \to n + \nu_e$ (and similar for muons), for cold neutron stars (temperature T below the neutrino opacity criterion $T < T_\nu \sim 1$ MeV) implies

$$\mu_n - \mu_p = \mu_e = \mu_\mu \ .$$

The chemical potentials are defined as

$$\mu_i = \frac{\partial \varepsilon_i}{\partial n_i} = \frac{\partial}{\partial x_i} E_i(n, \{x_j\}) \ , \quad i, j = n, p, e, \mu \ ,$$

where $\varepsilon_i = n \ E_i(n, \{x_j\})$ is the partial energy density of species i in the system. From the above equations:

$$\mu_e = 4(1 - 2x) E_s(n) \ .$$

Since electrons in neutron star interiors are ultrarelativistic,

$$\mu_e = \sqrt{p_{F,e}^2 + m_e^2} \approx p_{F,e}, \text{ and } p_{F,e} = (3\pi^2 n_e)^{1/3} = (3\pi^2 n)^{1/3} (x - x_\mu)^{1/3} \ ,$$

$$\frac{x - x_\mu}{(1 - 2x)^3} = \frac{64 E_s^3(n)}{3\pi^2 n} \ , \qquad (x - x_\mu)^{2/3} - x_\mu^{2/3} = \frac{m_\mu^2}{(3\pi^2 n)^{2/3}} \ .$$

The total pressure is then given as $P(n) = n^2 \left(\frac{\partial E_{\rm tot}}{\partial n} \right) \ .$

NJL model with multiquark interactions

$$\mathcal{L} = \bar{q}(i\partial\!\!\!/ - m)q + \mu_q \bar{q}\gamma^0 q + \mathcal{L}_4 + \mathcal{L}_8\ ,\ \ \mathcal{L}_4 = \frac{g_{20}}{\Lambda^2}[(\bar{q}q)^2 + (\bar{q}i\gamma_5\tau q)^2] - \frac{g_{02}}{\Lambda^2}(\bar{q}\gamma_\mu q)^2\ ,$$

$$\mathcal{L}_8 = \frac{g_{40}}{\Lambda^8}[(\bar{q}q)^2 + (\bar{q}i\gamma_5\tau q)^2]^2 - \frac{g_{04}}{\Lambda^8}(\bar{q}\gamma_\mu q)^4 - \frac{g_{22}}{\Lambda^8}(\bar{q}\gamma_\mu q)^2[(\bar{q}q)^2 + (\bar{q}i\gamma_5\tau q)^2]$$

Meanfield approximation: $\mathcal{L}_{\rm MF} = \bar{q}(i\partial\!\!\!/ - M)q + \tilde{\mu}_q\bar{q}\gamma^0 q - U\ ,$

$$M = m + 2\frac{g_{20}}{\Lambda^2}\langle\bar{q}q\rangle + 4\frac{g_{40}}{\Lambda^8}\langle\bar{q}q\rangle^3 - 2\frac{g_{22}}{\Lambda^8}\langle\bar{q}q\rangle\langle q^\dagger q\rangle^2\ ,$$

$$\tilde{\mu}_q = \mu_q - 2\frac{g_{02}}{\Lambda^2}\langle q^\dagger q\rangle - 4\frac{g_{04}}{\Lambda^8}\langle q^\dagger q\rangle^3 - 2\frac{g_{22}}{\Lambda^8}\langle\bar{q}q\rangle^2\langle q^\dagger q\rangle\ ,$$

$$U = \frac{g_{20}}{\Lambda^2}\langle\bar{q}q\rangle^2 + 3\frac{g_{40}}{\Lambda^8}\langle\bar{q}q\rangle^4 - 3\frac{g_{22}}{\Lambda^8}\langle\bar{q}q\rangle^2\langle q^\dagger q\rangle^2 - \frac{g_{02}}{\Lambda^2}\langle q^\dagger q\rangle^2 - 3\frac{g_{04}}{\Lambda^8}\langle q^\dagger q\rangle^4\ .$$

Thermodynamic Potential:

$$\Omega = U - 2N_f N_c \int \frac{d^3p}{(2\pi)^3}\left\{E + T\log[1 + e^{-\beta(E-\tilde{\mu}_q)}] + T\log[1 + e^{-\beta(E+\tilde{\mu}_q)}]\right\} + \Omega_0$$

S. Benic - Eur.Phys.J. A50 (2014) 111, arXiv:1401.5380

Neutron Star Cooling Processes

Process Name	Process	Emissivity Q_ν (erg cm^{-3} s^{-1})	Reference
Bremsstrahlung	$n + n \rightarrow n + n + \nu_e + \bar{\nu}_e$	$\simeq 10^{19} T_9^8$	Page, Geppert
	$n + p \rightarrow n + p + \nu_e + \bar{\nu}_e$		and Weber [92]
	$p + p \rightarrow p + p + \nu_e + \bar{\nu}_e$		
Modified Urca	$n + n \rightarrow n + p + e^- + \bar{\nu}_e$	$\simeq 10^{20} T_9^8$	Friman
	$n + p + e^- \rightarrow n + n + \nu_e$		and Maxwell [93]
Direct Urca	$n \rightarrow p + e^- + \bar{\nu}_e$	$\simeq 10^{27} T_9^6$	Lattimer et al. [94]
	$p + e^- \rightarrow n + \nu_e$		
Quark Urca	$d \rightarrow u + e^- + \bar{\nu}_e$	$\simeq 10^{26} \alpha_c T_9^6$	Iwamoto [95]
	$u + e^- \rightarrow d + \nu_e$		
Kaon Condensate	$n + K^- \rightarrow n + e^- + \bar{\nu}_e$	$\simeq 10^{24} T_9^6$	Brown et al. [96]
	$n + e^- \rightarrow n + K^- + \nu_e$		
Pion Condensate	$n + \pi^- \rightarrow n + e^- + \bar{\nu}_e$	$\simeq 10^{26} T_9^6$	Maxwell et al. [97]
	$n + e^- \rightarrow n + \pi^- + \nu_e$		

Direct Urca is the fastest cooling process.
Threshold for onset: $p_{F,n} < p_{F,p+}\ p_{F,e}$. For electrons only then x_{DU}=1/9.

Neutron Star Cooling Processes

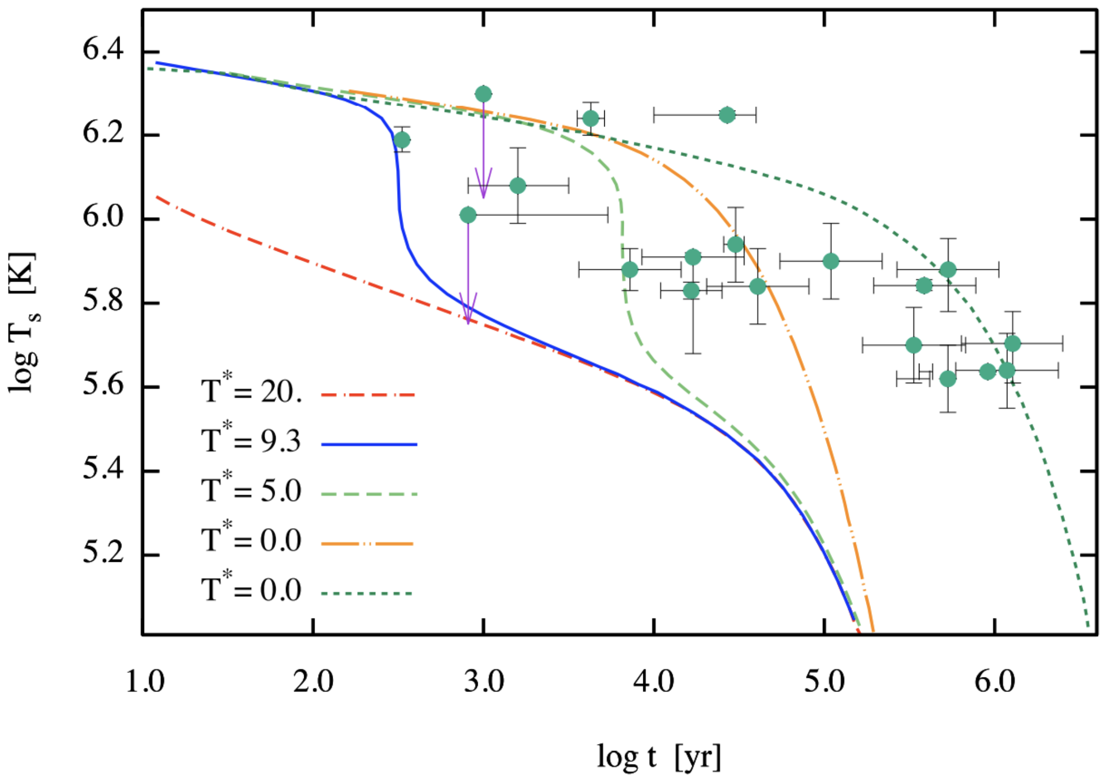

Figure 6. Cooling tracks of compact stars with quark cores in the surface-temperature–age diagram. The masses of the stars are the same, $M = 1.93\ M_\odot$, and the different curves correspond to different values of the parameter T^* in units of keV, except the dotted line, which corresponds to $1\ M_\odot$ mass nucleonic compact star without a quark core. The observational points with error bars are shown by green circles; the arrows show the upper limits on surface temperatures of known objects.

Armen Sedrakian - Particles 2023, 6(3), 713-730 - arXiv - 2306.13884